Appl Biochem Biotechnol (2009) 155:304–313
DOI 10.1007/s12010-008-8362-5

Purification and Characterization of a Glycoside Hydrolase Family 43 β-xylosidase from *Geobacillus thermoleovorans* IT-08

Kurt Wagschal · Chamroeun Heng · Charles C. Lee · George H. Robertson · William J. Orts · Dominic W. S. Wong

Received: 15 May 2008 / Accepted: 4 September 2008 /
Published online: 26 September 2008

Abstract The gene encoding a glycoside hydrolase family 43 β-xylosidase (GbtXyl43A) from the thermophilic bacterium *Geobacillus thermoleovorans* strain IT-08 was synthesized and cloned with a C-terminal His-tag into a pET29b expression vector. The recombinant gene product termed GbtXyl43A was expressed in *Escherichia coli* and purified to apparent homogeneity. Michaelis–Menten kinetic parameters were obtained for the artificial substrates *p*-nitrophenyl-β-D-xylopyranose (4NPX) and *p*-nitrophenyl-α-L-arabinofuranose (4NPA), and it was found that the ratio k_{cat}/K_m 4NPA/k_{cat}/K_m 4NPX was ~7, indicting greater catalytic efficiency for 4NP hydrolysis from the arabinofuranose aglycon moiety. Substrate inhibition was observed for the substrates 4-methylumbelliferyl xylopyranoside (muX) and the arabinofuranoside cogener (muA), and the ratio k_{cat}/K_m muA/k_{cat}/K_m muX was ~5. The enzyme was competitively inhibited by monosaccharides, with an arabinose K_i of 6.8±0.62 mM and xylose K_i of 76±8.5 mM. The pH maxima was 5.0, and the enzyme was not thermally stable above 54 °C, with a $t_{1/2}$ of 35 min at 57.5 °C. GbtXyl43A showed a broad substrate specificity for hydrolysis of xylooligosaccharides up to the highest degree of polymerization tested (xylopentaose), and also released xylose from birch and beechwood arabinoxylan.

Keywords Arabinofuranosidase · Xylosidase · Glycoside hydrolase family 43 · Hemicellulose degradation · Substrate inhibition

Introduction

Renewable energy resources are becoming increasingly important due to their being both locally produced and overall more environmentally benign than current extractive energy sources. Lignocellulosic plant biomass is composed mainly of cellulose, lignin, and

K. Wagschal (✉) · C. Heng · C. C. Lee · G. H. Robertson · W. J. Orts · D. W. S. Wong
Western Regional Research Center, USDA Agricultural Research Service, 800 Buchanan Street, Albany, CA 94710, USA
e-mail: kurt.wagschal@ars.usda.gov

hemicellulose, with xylan being the main component of hemicellulose. Structurally, xylans are heteropolysaccharides consisting of a linear β-D-(1→4)-linked xylopyranoside backbone that is variously substituted with arabinose and other substituents depending on the biomass source. The xylose backbone of cereal xylans can be substituted with (1→2)- and/or (1→3)-linked α-L-arabinofuranosyl, α-D-glucuronic acid, and *O*-2- and/or *O*-3-linked acetate groups. Moreover, the α-L-arabinofuranose branch residues can themselves be esterified with ferulate and *p*-coumarate residues, which may in turn be cross-linked as well as be oxidatively coupled to lignin. The cost-effective production of fuels and chemical feedstocks from biomass will involve the deconstruction of both the cellulosic and hemicellulosic components. Due to the complexity of xylan, its deconstruction requires the concerted action of several enzymes with the ability to hydrolyze the various hemicellulose linkages [1–3]. In conjunction with β-xylanases, which have endo-xylanolytic activity, β-xylosidases are essential in completely depolymerizing xylan. β-xylosidases (EC 3.2.1.37) are exo-type glycosidases that catalyze the successive removal of β-xylosyl residues from the nonreducing termini of xylobiose and higher linear β-1,4-xylooligosaccharides, and they are found in GH families 3, 30, 39, 43, 51, 52, and 54 [1, 3]. D-xylopyranose and L-arabinofuranose are spatially similar such that the glycosidic bonds and hydroxyl groups can be overlaid, leading to bifunctional xylosidase–arabinofuranosidase enzymes [4–6].

Thermophilic organisms are a natural repository of many biotechnologically valuable enzyme activities [7], and areas of the earth where geothermal activity occurs have frequently been a source of these organisms. Thus, a thermally stable xylanase has previously been found in *Bacillus thermoleovorans* K-3d isolated from a hot spring in Japan [8], and a thermophilic lipase has been cloned from *B. thermoleovorans* ID-1 isolated from a hot spring in Indonesia [9]. Recently, a xylanolytic gene cluster from the thermophilic bacterium *Geobacillus thermoleovorans* IT-08 was isolated that contains a number of potentially useful hemicellulolytic enzymes [10]. Preliminary X-ray analysis was performed on a glycosyl hydrolase family 43 β-xylosidase from this cluster (GenBank accession DQ345777) [11], and we report here the detailed biochemical characterization of this enzyme termed GbtXyl43A.

Materials and Methods

GbtXyl43A Expression and Purification

The nucleotide sequence encoding GbtXyl43A was synthesized (BioBasic, Markham, Ontario, Canada) and subcloned into the 5′*Nde*I and 3′ *Xho*I sites of a pET29b(+) expression plasmid (EMD Biosciences, San Diego, CA, USA) to yield the GbtXyl43A gene with an N-terminal His_6-tag. The host *Escherichia coli* BL21(DE3) was transformed with the expression plasmid containing the GbtXyl43A insert, streaked onto Luria–Bertani agar plates amended with 30 μg/ml kanamycin (Research Products International, Mount Prospect, IL, USA), and incubated overnight at 37 °C. Positive transformants were selected based on enzymatic hydrolysis of *p*-nitrophenyl-α-L-arabinofuranose (4NPA) (described below) and restriction digestion of the plasmids. A glycerol stock stab was used to inoculate a 100-ml seed culture of *E. coli*, which was then grown in Terrific Broth (Research Products International) amended with 30 μg/ml kanamycin (TB_{kan}) broth at 37 °C at 250 rpm for 16 h. A 100-ml aliquot was used to inoculate 1,000 ml TB_{kan}, which was grown at 37 °C to $OD_{600\ nm}$=2–3. Then, the culture was cooled before inducing protein expression with 0.5 mM IPTG, and incubation was allowed to proceed at 25 °C at 170 rpm overnight (~16 h). 400–500-ml aliquots were

pelletted, and the pellets stored frozen at −80 °C. Cell lysis and release of soluble proteins was achieved by adding to each pellet 65 mL solution containing 65 ml CelLytic B cell lysis reagent, 0.5 mg/ml hen egg-white lysozyme, 2 mM β-mercaptoethanol (BME), 5 U/mL Benzonase (all from Sigma-Aldrich, St. Louis, MO, USA), and 1 μL/ml CalBiochem protease inhibitor cocktail III (EMD Biosciences). Cells were incubated with tube rotation on a Lab-Quake (Barnstead/Thermolyne, Dubuque, IA, USA) in the lysis solution for 30 min at room temperature, cooled to 0–4 °C, and centrifuged to remove cell debris. The protein was purified using Ni-NTA resin (Qiagen, Valencia, CA, USA) according to the manufacturer's instructions by first adjusting the supernatant solution to 300 mM NaCl, 25 mM imidazole, 2 mM BME, and 50 mM phosphate buffer (pH 8.0) before loading onto a Ni-NTA column. The composition of the wash buffer used was 50 mM phosphate buffer (pH 8.0) containing 10% glycerol, 2 mM BME, 1 μL/ml protease inhibitor cocktail III, 300 mM NaCl, and 25 mM imidazole. The protein was eluted using the same buffer except that the imidazole concentration was increased to 250 mM. Ni-NTA column fractions were analyzed by PAGE and those containing the enzyme were pooled and purified to apparent homogeneity by size exclusion chromatography using a Superdex 200 16/60 column (GE Life Sciences) using a flow rate of 0.3 ml/min and a running buffer consisting of 50 mM phosphate buffer (pH 6.2) containing 150 mM NaCl and 10% glycerol. Protein concentrations were determined using Coomassie Plus reagent (Pierce Biotechnology, Rockford, IL, USA) following the manufacturer's protocol. Enzyme fractions were analyzed using PAGE following the manufacturer's protocol (Invitrogen, Carlsbad, CA, USA).

Activity vs pH Profile

The effect of pH on the apparent V_{max} (Fig. 1) was measured using endpoint assays utilizing an equal volume of 1 M Na_2CO_3 to quench the reactions and raise all the pH values to ~pH 11. Reaction conditions were 40 °C, 4 mM *p*-nitrophenyl-β-D-xylopyranose (4NPX), 0.1% bovine serum albumin (BSA; Sigma), and 100 mM citrate for pH 3 to pH 6.5, 100 mM phosphate for pH 6.5 to pH 8.0, and 100 mM AMPSO for pH 8.0 to pH 9.5.

Enzyme Assays

For assays using 4-nitrophenyl-β-D-xylopyranoside and 4-nitrophenyl-α-L-arabinofuranoside glycosides as substrates (4NPX and 4NPA, respectively; Sigma), the enzyme activity

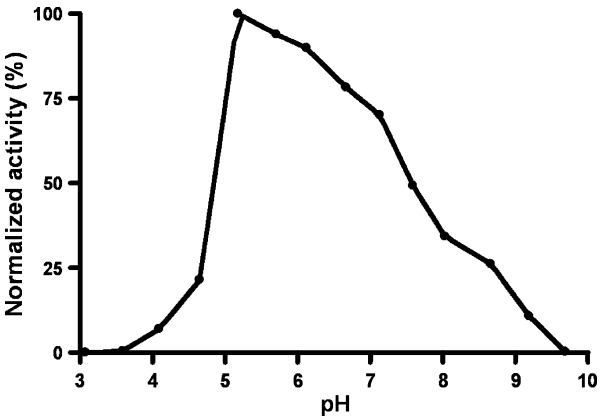

Fig. 1 Relative enzyme activity at the indicated pH values. Enzyme activity was determined with 4 mM 4NPX (*dots*). Reaction conditions were as described in the "Materials and Methods" section

was determined by measuring the change in absorbance at 400 nm due to NP release using a Spectramax M2 spectrophotometer equipped with a temperature controller (Molecular Devices, Sunnyvale, CA, USA). For assays using 4-methylumbelliferyl-β-D-xylopyranoside (muX) and 4-methylumbelliferyl-α-L-arabinofuranoside (muA) as substrates (Sigma), the enzyme activity was determined by measuring the change in fluorescence using an excitation wavelength of 349 nm and an emission wavelength of 460 nm. Xylobiose (X2) and xylotriose (X3) (Wako Chemicals USA, Richmond, VA, USA) were assayed using a spectrophotometric enzyme-coupled assay as previously described [12]. In a typical kinetic assay 240 μL of 50 mM phosphate buffer (pH 6.2) containing 0.1% BSA and varying substrate concentrations was preincubated at 40 °C for 5 min, then a 10-μL enzyme solution was added and mixed to initiate the reaction. Generally, 16 different substrate concentrations, each in quadruplicate, were used to assess the kinetic parameters reported in Table 1. To accurately obtain the kinetic parameters for each substrate, the concentration of GbtXyl43A was chosen so that the proportion of substrate hydrolyzed at the end of the data acquisition period generally ranged from <1% to 10%; 70 nM for 4NPA, 180 nM for 4NPX, 50 nM for muA, 180 nM for muX, 200 nM for X2, and 800 nM for X3. The kinetic parameters k_{cat} and K_m in Table 1 for the NP substrates were calculated by nonlinear regression fitting of the data to the Michaelis–Menten equation using the program GraFit 5 (Erithacus Software, Surrey, UK). For the methylumbelliferyl substrates, which exhibited substrate inhibition (Fig. 3), the data was fitted to Eq. 1, derived from an uncompetitive substrate inhibition model, using GraphPad Prism 4 (GraphPad Software, San Diego, CA, USA):

$$v_0 = \frac{k_{cat} \times [E_0] \times [S]}{K_m + [S] + \left(S^2/K_i\right)} \quad (1)$$

The inhibition constant K_i for arabinose was determined using a kinetic spectrophotometric assay wherein velocity was measured in the absence of added monosaccharide, and then in the presence of 5, 15, 30, 75, and 150 mM arabinose using 4NPA as the substrate at concentrations ranging from 24 to 6,400 μM in a reaction buffer consisting of 50 mM PO_4 (pH 6.2), 0.1% BSA, and 50 nM GbtXyl43A. Arabinose at the various concentrations and GbtXyl43A were preincubated in the assay buffer for 10 min at 40 °C, and the reaction was initiated by adding the substrate. The K_i for xylose was similarly obtained employing

Table 1 Michaelis–Menten Kinetic parameters for substrate hydrolysis by GbtXyl43A.

Substrate[a]	Concentration range (mM)	K_m (mM)	k_{cat} (s^{-1})	k_{cat}/K_m (mM^{-1} s^{-1})
4NPA[b]	0.048–9.6	0.497±0.033	1.18±0.02	2.37±0.16
4NPX[b]	0.024–9.6	0.550±0.080	0.18±0.01	0.33±0.05
muA[c]	0.006–8	0.081±0.006	0.233±0.008	2.88±0.24
muX[c]	0.006–12	0.366±0.069	0.208±0.025	0.57±1.5
X2[b]	2–96	12.8±0.93	0.065±0.002	0.0051±0.0004
X3[b]	1–72	5.09±0.47	0.020±0.001	0.0039±0.0004

[a] Reaction conditions were 50 mM PO_4, pH 6.2, 40 °C, 0.1% BSA, and GbtXyl43A concentrations as described in the text.

[b] Parameters obtained from nonlinear regression fitting to the Michaelis–Menten equation.

[c] Parameters obtained from nonlinear regression fitting to Eq. 1 derived from a substrate uncompetitive inhibition model. K_i (muA)=840±60 μM, K_i (muX)=840±160 μM.

xylose concentrations of 25, 50, 100, 200, and 400 mM, 4NPX concentrations from 24 μM to 3,200 μM, and 50 nM GbtXyl43A. The K_i values were calculated by nonlinear curve fitting of the data to a competitive inhibition model using GraphPad Prism 4 (GraphPad Software).

Thermal Inactivation Half-Life

Irreversible thermal denaturation half-life was measured by placing 120-μL aliquots of 260 nM GbtXyl43A in an assay buffer consisting of 50 mM phosphate, pH 6.2, and 0.1% BSA in a PCR plate, and incubating on an MJ Research PTC-200 thermocycler (Bio-Rad, Hercules, CA, USA) set to a temperature gradient of 40 °C to 57.5 °C using a nonheated cover. Aliquots were taken at specific time points and placed on ice before assaying. To assay, aliquots of the enzyme from the various time points were transferred to 150 μL assay buffer and preincubated at 40 °C for 10 min to allow refolding, 4NPA substrate was added to a final concentration of 4 mM, and the change of absorbance at 400 nm due to 4NP release was measured using a Spectramax M3 plate reader (Molecular Devices). Half-lives of thermal inactivation were calculated using $t_{1/2} = \ln 2/k_{inact}$, where k_{inact} is the inactivation rate constant obtained from the slope by plotting log (residual activity/initial activity) vs time (Fig. 2).

Substrate Specificity

Thin-layer chromatography (TLC) was used to monitor the degradation of the following natural polymeric substrates: xylobiose, xylotriose (both from Wako Chemicals USA), xylotetraose, xylopentaose, sugar beet arabinan, debranched sugar beet arabinan, wheat medium viscosity arabinoxylan, (all from Megazyme, Wicklow, Ireland), oat spelt xylan, birchwood xylan, and beechwood xylan (all from Sigma). The composition of these natural substrates as specified by the supplier and by gas–liquid chromatography (GLC) analysis are as follows. The sugar beet arabinan substrate consisted of a 1,5-α-linked arabinose backbone to which 1,3-α-linked and possibly some 1,2-α-linked L-arabinofuranosyl groups were attached. Approximately 60% of the main-chain arabinofuranosyl residues were

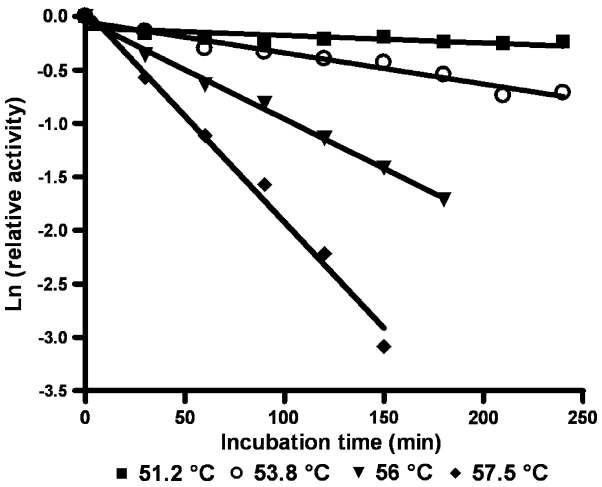

Fig. 2 Effect of temperature on the $t_{1/2}$ for thermal denaturation of deAX at the indicated temperatures. Reaction conditions were as described in the "Materials and Methods" section

substituted by single 1,3-linked arabinofuranosyl groups. The debranched sugar beet arabinan employed was prepared by the manufacturer such that all 1,2- and 1,3-α-linked L-arabinofuranosyl branch units were removed. The cereal grain natural arabinoxylan substrates had homopolymeric backbones of (1–4)-β-D-xylopyranosyl residues substituted with (1–2)- and/or (1–3)-α-linked L-arabinofuranosyl branch units. The wheat arabinan medium viscosity arabinoxylan had an arabinose–xylose–other sugars ratio of ~37:61:2, and the oat spelt xylan had an arabinose–xylose–glucose ratio of ~10:75:15. The xylans from the two hardwood substrates birchwood and beechwood were each specified as containing >90% xylose residues. In-house GLC analysis of trifluoroacetic acid hydrolsylates of the beechwood and birchwood xylan used showed that each contained about 0.5% (dry-weight basis) arabinose. Reaction conditions were 180 min incubations at 45 °C in 120 μL of reaction buffer containing 10 mM phosphate, pH 6.2, natural substrate concentration of 4 mg/ml for the arabinans and arabinoxylans or 2.5 mg/ml for the xylooligosaccharides, 55 μM GbtXyl43A for the hydrolysis reactions, and no enzyme for parallel no-enzyme incubations. TLC was performed using high-performance TLC silica plates (Alltech, Waukegan, IL, USA), with mobile phase composition EtOAc–MeOH–H_2O 7:2:1, and carbohydrates were visualized using 20% H_2SO_4 in MeOH containing 1 mg/ml orcinol (Aldrich) followed by gentle heat.

Results and Discussion

Analysis of the GbtXyl43A Gene

Due to the structural complexity of xylans, where the β-1,4-xylose backbone is variously substituted with L-arabinofuranosyl, glucuronyl, 4-*O*-methylglucuronyl, and acetyl groups, as well as being cross-linked through ferulate groups, the genes encoding the components of xylan degradation pathways are known to be coordinately synthesized in bacterial species [13, 14], and GbtXyl43A was one member of a xylanolytic gene cluster that also included another putative exo-xylanase GH family 43 protein (NCBI accession DQ387047), as well as a putative GH family 51 arabinofuranosidase (abfa; NCBI accession DQ387046). The gene encoding GbtXyl43A consisted of an open reading frame of 1,536 nucleotides encoding a nascent polypeptide of 511 amino acids with a predicted molecular weight of 58.1 kDa. Phylogenetic analysis of the evolutionary relationship of the amino acid sequence of GbtXyl43A to other GH's places GbtXyl43A in GH family 43 in the CAZY database (http://www.cazy.org/) [15], with closest relation to a putative β-xylosidase/α-arabinofuranosidase from *Oceanobacillus iheyensis* (56% consensus, 44% identical; NCBI accession BAC14043) [16], an α-arabinofuranosidase (deAFc; 55% consensus, 44% identical; NCBI accession ABB92159) [17] and a β-xylosidase/α-arabinofuranosidase (deAX; 54% consensus, 42% identity; NCBI accession EU636010) [18], both isolated from a commercial compost starter mixture, and a putative β-xylosidase from *Clostridium phytofermentans* (57% consensus, 43% identical; NCBI accession ABX42396). Members of GH family 43 are known to catalyze glycosidic bond hydrolysis resulting in inversion at the anomeric center [19–21]. In the case of inverting hydrolytic enzymes, a single-displacement reaction ensues [22], in which one active site carboxylate provides general base catalytic assistance to the attack of water, while another carboxylic acid provides general acid catalytic assistance to cleaving of the glycosidic bond [23]. GbtXyl43A is similar to a GH family 43 β-D-xylosidase XynB3 from *Geobacillus stearothermophilus* T-6 (47% consensus, 33% identical; NCBI accession ABI49959) for which the catalytic active site residues have been identified [24]. Alignment of the amino

acid sequences of GbtXyl43A and XynB3 reveals high homology around the active-site residues, with Asp14 predicted to be the general base (aligns with Asp 15 in XynB3) and Glu177 predicted to be the general acid residue (aligns with Glu187 in XynB3), while Asp 121 (aligns with Asp 128 in XynB3) is predicted to be an invariant Asp residue found in all GH family 43 enzymes, where it serves to modulate the pKa and orientation of the general acid residue, as well as contributing to substrate binding and transition state stabilization [25].

Enzyme Properties

The GH43 hemicellulolytic enzymes in general are highly promising candidates for the critical β-xylosidase activity, as they do not exhibit transglycosylation at high substrate concentrations, and the most catalytically efficient xylosidase characterized to date falls into this class [26]. The activity of GbtXyl43A was found to have a pH maximum occurring at pH 5.0 (Fig. 1). The pH maxima was also found to be roughly the same for the similar enzymes deAFc (broad pH maxima , pH 5 to pH 8.5; 55% amino acid sequence consensus) [17] and deAX (pH maxima 6; 54% amino acid sequence consensus) [18]. These GH 43 enzymes all have pH maxima that center slightly below neutrality, and in the event a dilute acid pretreatment step is envisioned, it may be highly desirable to discover enzyme engineering targets for GH43 enzymes that result in lower pH optima. The $t_{1/2}$ for thermal denaturation was calculated to be 970 min at 51.2 °C, 240 min at 53.8 °C, 75 min at 56 °C, and 35 min at 57.5 °C (Fig. 2). The kinetic parameters for hydrolysis of 4NPA, 2NPX, 4NPX, muA, muX, xylobiose, and xylotriose are shown in Table 1. When comparing 4-NP aglycon synthetic substrates, k_{cat} was significantly larger for the arabinofuranoside substrate; k_{cat} 4NPA/4NPX=6.6, while the K_m values were quite similar. As a result, GbtXyl43A showed a seven-fold greater catalytic efficiency factor k_{cat}/K_m for 4NPA substrate hydrolysis compared to 4NP hydrolysis from the xylopyranosyl moiety. GbtXyl43A showed substrate inhibition when 4-methylumbelliferyl was the aglycon group. Figure 3 shows nonlinear regression fitting of the data to Eq. 1, derived from an uncompetitive inhibition model [27], for hydrolysis of muA (Fig. 3a; R^2=0.99) and muX (Fig. 3b; R^2=0.99). The K_i for muA was 840±60 μM, and that for muX was 840±160 μM. The insets on panels a and b in Fig. 3 show biphasic Hill plots, log $v/(V_{max}-v)=h$ log[S], which corroborate this inhibition scheme, where at high substrate concentrations, a second molecule of substrate is able to bind and form an unproductive ES_2 complex, with the slope on the Hill plots then becoming −0.92 for muA and −0.92 for muX. Unlike the result obtained for the 4NPA and 4NPX substrates, k_{cat} values were equal for both muX and muA, while K_m muX/K_m muA was ~5. The aglycon 4-methylumbelliferyl group appears to show a propensity for binding of a second substrate molecule in the active site leading to substrate inhibition, since the similar β-xylosidase/arabinofuranosidase enzyme deAX also showed substrate inhibition with muA (K_i 410 μM) and muX (K_i 1,020 μM) [18], as did deAFc with muX (muA was not tested), where the K_i was on the order of 3 mM [17]. Hydrophobic interactions are an important component of protein–carbohydrate complexes [28], and the moderately hydrophobic character of the umbelliferyl group, as well as the way muA or muX pack in the active site, may be responsible for the observed substrate inhibition propensity. The crystal structure of the related substrate 4-methylumbelliferyl-β-D-glucopyranoside shows that the umbelliferyl moiety is essentially planar, and the structure appears as layers of hydrophobic and hydrophilic regions that each display strong intermolecular interactions [29]. Hydrophobicity has been attributed to the +1 aglycon binding subsite of a GH 43 xylosidase from *G. stearothermophilus* T-6 based on Brønsted coefficients for hydrolysis of 2-aryloxytetrahydropyrans in the active site compared to that

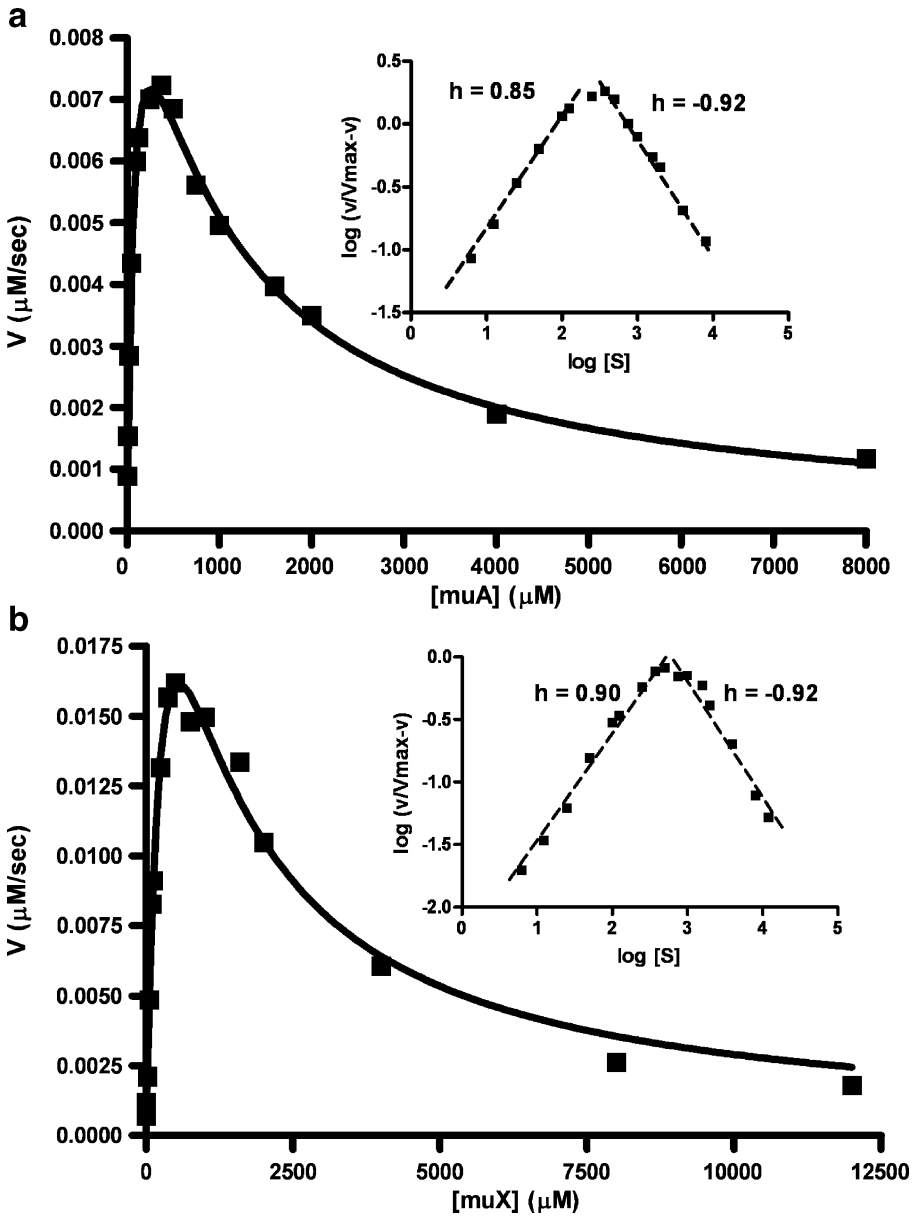

Fig. 3 Steady state kinetics for the enzyme-catalyzed hydrolysis of muA (**a**) and muX (**b**); *insets* are Hill plots of the data

in solution [24]. Moreover, crystal structures have revealed the presence of conserved Trp and Phe hydrophobic residues at the +1 sugar subsite in GH 43 enzymes [25]. In summary, for the synthetic substrates, GbtXyl43A showed significantly greater catalytic efficiency for cleavage of 4NP or mu from the arabinofuranose substrates compared to the xylopyranoside substrates.

Since monosaccharide sugar concentrations can reach 0.3–3 M during saccharification of biomass, the ability of arabinose and xylose to competitively inhibit GbtXyl43A was tested. The K_i for arabinose obtained using 4NPA as the substrate was 6.8±0.62 mM (R^2=0.99), and the K_i for xylose obtained using 4NPX as the substrate was 76±8.5 mM (R^2=0.98). The K_i for arabinose for the arabinofuranosidase deAFc was 27 mM [17], the K_i for arabinose for the β-xylosidase/arabinofuranosidase deAX was 18.5 mM [18], and the K_i for arabinose for a catalytically efficient GH 43 enzyme isolated from *Selenomonas ruminantium* was on the order of 50–60 mM [30]. Thus, GbtXyl43A appears to be more highly inhibited by arabinose than some other GH family 43 enzymes. The K_i of GbtXyl43A for xylose is, by contrast, ~11-fold higher than that for arabinose, and this may reflect a less favorable environment for binding of the xylopyranosyl ring in the active site.

GH 43 enzymes are known to show broad specificity at the −1 subsite of the active site, which binds the substrate glycon [31], with examples of GH 43 enzyme types including β-xylosidases, arabinofuranosidases, bifunctional xylosidases/arabinofuranosidases, xylanases, and arabinases [3]. Concerning synthetic substrate specificity, GbtXyl43A hydrolyzed both arabinofuranosyl and xylopyranosyl synthetic aryl substrates and actually exhibited a greater catalytic efficiency for arabinofuranosyl synthetic substrates. D-Xylopyranose and L-arabinofuranose are spatially similar, thereby rationalizing the existence of bifunctional α-L-arabinofuranosidases/β-D-xylosidases with respect to synthetic substrate hydrolysis. Concerning hydrolysis of the corresponding native glycosidic bonds, arabinose was not released from either debranched sugar beet arabinan or sugar beet arabinan. Moreover, neither arabinofuranosidase nor xylosidase activity was observed when arabinoxylans from either wheat or oat were tested. Release of xylose was observed from birch and beech arabinoxylan, both of which have very little arabinofuranosyl substitution of the polymeric xylose backbone [32]. While GbtXyl43A was able to hydrolyze xylobiose and xylotriose, the k_{cat} values of 0.065 s^{-1} and 0.020 s^{-1}, respectively, were very low and the K_m values were 5 mM and ~13 mM, respectively, resulting in exceedingly low catalytic efficiency factors for xylooligosaccharide hydrolysis. When xylobiose, xylotriose, xylotetraose, and xylopentaose were tested for activity by TLC, it was observed that GbtXyl43A was capable of converting all of the xylooligosaccharide substrates tested to xylose. Thus, GbtXyl43A function appears to be limited to exo-xylosidase activity for natural substrate hydrolysis and does not appear to have significant arabinofuranosidase activity on natural substrates. This result clearly shows that the natural substrate specificity cannot be inferred from synthetic substrate specificity since GbtXyl43A actually exhibited greater catalytic efficiency for hydrolyzing NP from arabinofuranosyl synthetic substrates. In contrast to the narrow natural substrate specificity of GbtXyl43A, the similar enzyme deAX displayed debranching and exo-arabinofuranosidase activity on arabinan, short arabinooligosaccharides, and arabinoxylan from wheat and rye, while also displaying xylosidase activity on xylooligosaccharides and arabinoxylan from birch and beechwood [18]. Since GbtXyl43A was found in a xylanolytic gene cluster that also included a putative GH family 51 arabinofuranosidase (abfa; NCBI accession DQ387046), characterization of this latter protein may reveal the necessary arabinofuranosidase activity required for an arabinoxylan deconstruction metabolic pathway in *G. thermoleovorans* IT-08.

Acknowledgements Reference to a company and/or products is for purposes of information and does not imply approval or recommendation of the product to the exclusion of others that may also be suitable. All programs and services of the U.S. Department of Agriculture are offered on a nondiscriminatory basis without regard to race, color, national origin, religion, sex, age, marital status, or handicap.

References

1. Biely, P. (2003). In J. R. Whitaker, A. G. J. Voragen, & D. W. S. Wong (Eds.), *Handbook of food enzymology* pp. 879–915. New York: Marcel Dekker.
2. Saha, B. C. (2003). *Journal of Industrial Microbiology & Biotechnology*, *30*, 279–291. doi:10.1007/s10295-003-0049-x.
3. Shallom, D., & Shoham, Y. (2003). *Current Opinion in Microbiology*, *6*, 219–228. doi:10.1016/S1369-5274(03)00056-0.
4. Jordan, D. B., & Li, X. -L. (2007). *Biochimica et Biophysica Acta*, *1774*, 1192–1198.
5. Mai, V., Wiegel, J., & Lorenz, W. W. (2000). *Gene*, *247*, 137–143. doi:10.1016/S0378-1119(00)00106-2.
6. Lee, R. C., Hrmova, M., Burton, R. A., Lahnstein, J., & Fincher, G. B. (2003). *The Journal of Biological Chemistry*, *278*, 5377–5387. doi:10.1074/jbc.M210627200.
7. Haki, G. D., & Rakshit, S. K. (2003). *Bioresource Technology*, *89*, 17–34. doi:10.1016/S0960-8524(03)00033-6.
8. Sunna, A., Prowe, S. G., Stoffregen, T., & Antranikan, G. (1997). *FEMS Microbiology Letters*, *148*, 209–216. doi:10.1111/j.1574-6968.1997.tb10290.x.
9. Cho, A.-R., Yoo, S.-K., & Kim, E.-J. (2000). *FEMS Microbiology Letters*, *186*, 235–238. doi:10.1111/j.1574-6968.2000.tb09110.x.
10. Puspaningsiha, N.N.T. (2004). PhD thesis, Bogor Agricultural University, Indonesia.
11. Rohman, A., Oosterwijk, N. V., Kralj, S., Dijkhuizen, L., Dijkstrab, B. W., & Puspaningsiha, N. N. T. (2007). *Acta Crystallographica*, *F63*, 932–935.
12. Wagschal, K., Franqui-Espiet, D., Lee, C. C., Robertson, G. H., & Wong, D. W. S. (2005). *Applied and Environmental Microbiology*, *71*, 5318–5323. doi:10.1128/AEM.71.9.5318-5323.2005.
13. Tsujibo, H., Kosaka, M., Ikenishi, S., Sato, T., Katsushiro, M., & Inamori, Y. (2004). *Journal of Bacteriology*, 186, 1029–1037. doi:10.1128/JB.186.4.1029-1037.2004.
14. Shulami, S., Gat, O., Sonenshein, A. L., & Shoham, Y. (1999). *Journal of Bacteriology*, *181*, 3695–3704.
15. Coutinho, P. M., & Henrissat, B. (1999). In H. J. Gilbert, et al. (Ed.), *Recent Advances in carbohydrate bioengineering* pp. 3–12. Cambridge: The Royal Society of Chemistry, Cambridge.
16. Takami, H., Takaki, Y., & Uchiyama, I. (2002). *Nucleic Acids Research*, *30*, 3927–3935. doi:10.1093/nar/gkf526.
17. Wagschal, K., Franqui-Espiet, D., Lee, C. C., Kibblewhite-Accinelli, R. E., Robertson, G. H., & Wong, D. W. S. (2007). *Enzyme and Microbial Technology*, *40*, 747–753. doi:10.1016/j.enzmictec.2006.06.007.
18. Wagschal, K., Heng, C., Lee, C. C., & Wong, D. W. S. (2008). *Applied Microbiology and Biotechnology*. doi:10.1007/s00253-008-1662-4.
19. Pitson, S. M., Voragen, A. G. J., & Beldman, G. (1996). *FEBS Letters*, *398*, 7–11. doi:10.1016/S0014-5793(96)01153-2.
20. Braun, C., Meinke, A., Ziser, L., & Withers, S. G. (1993). *Analytical Biochemistry*, *212*, 259–262. doi:10.1006/abio.1993.1320.
21. Kersters-Hilderson, H., Claeyssens, M., Doorslaer, E. V., & Bruyne, C. K. D. (1976). *Carbohydrate Research*, *47*, 269–273. doi:10.1016/S0008-6215(00)84192-0.
22. Koshland, D. E. (1953). *Biological Reviews of the Cambridge Philosophical Society*, *28*, 416–436. doi:10.1111/j.1469-185X.1953.tb01386.x.
23. Ly, H. D., & Withers, S. G. (1999). *Annual Review of Biochemistry*, *68*, 487–522. doi:10.1146/annurev.biochem.68.1.487.
24. Shallom, D., Leon, M., Bravman, T., Ben-David, A., Zaide, G., Belakhov, V., et al. (2005). *Biochemistry*, *44*, 387–397. doi:10.1021/bi048059w.
25. Brüx, C., Ben-David, A., Shallom-Shezifi, D., Leon, M., Niefind, K., Shoham, G., et al. (2006). *Journal of Molecular Biology*, *359*, 97–109. doi:10.1016/j.jmb.2006.03.005.
26. Jordan, D. B., Li, X.-L., Dunlap, C. A., Whitehead, T. R., & Cotta, M. A. (2007). *Applied Biochemistry and Biotechnology*, *141*, 51–76. doi:10.1007/s12010-007-9210-8.
27. Malet, C., & Planas, A. (1997). *Biochemistry*, *36*, 13838–13848. doi:10.1021/bi9711341.
28. Quiocho, F. A. (1989). *Pure and Applied Chemistry*, *61*, 1293–1306. doi:10.1351/pac198961071293.
29. Roey, P. V., & Salerno, J. M. (1988). *Acta Crystallographica*, *C44*, 865–867.
30. Jordan, D. B., & Braker, J. D. (2007). *Archives of Biochemistry and Biophysics*, *465*, 231–246. doi:10.1016/j.abb.2007.05.016.
31. Davies, G. J., Wilson, K. S., & Henrissat, B. (1997). *The Biochemical Journal*, *321*, 557–559.
32. Timell, T. (1964). *Advances in Carbohydrate Chemistry and Biochemistry*, *19*, 247–299.